



Hot Brownian Motion

Daniel Rings, Romy Schachoff, Markus Selmke, Frank Cichos, and Klaus Kroy*

Institut für Theoretische Physik, Universität Leipzig, Postfach 100920, 04009 Leipzig, Germany
and Institut für Experimentelle Physik I, Universität Leipzig, Linnéstraße 5, 04103 Leipzig, Germany
 (Received 23 March 2010; revised manuscript received 8 July 2010; published 26 August 2010)

We derive the Markovian description for the nonequilibrium Brownian motion of a heated nanoparticle in a simple solvent with a temperature-dependent viscosity. Our analytical results for the generalized fluctuation-dissipation and Stokes-Einstein relations compare favorably with measurements of laser-heated gold nanoparticles and provide a practical rational basis for emerging photothermal tracer and nanoparticle trapping and tracking techniques.

DOI: 10.1103/PhysRevLett.105.090604

PACS numbers: 05.40.Jc, 05.70.Ln, 47.15.G–

Brownian motion is the erratic motion of suspended particles that are large enough to admit some hydrodynamic coarse-graining, yet small enough to exhibit substantial thermal fluctuations. Such mesoscopic dynamics is ubiquitous in the micro- and nanoworld, and, in particular, in soft and biological matter [1,2]. Since their first formulation more than a century ago [3], the laws of Brownian motion have therefore found so many applications and generalizations in all quantitative sciences that one may justly speak of a “slow revolution” [4]. In Langevin’s popular formulation they take the simple form of Newton’s equation of motion for a particle of mass m and radius R subject to a drag force $-\zeta_0 \mathbf{p}/m$ and a randomly fluctuating thermal force $\xi(t)$:

$$\dot{\mathbf{p}} + \zeta_0 \mathbf{p}/m = \xi \quad (t > 0). \quad (1)$$

As a cumulative representation of a large number of chaotic molecular collisions ξ is naturally idealized as a Gaussian random variable. Its variance is tied to the Stokes friction coefficient

$$\zeta_0 = 6\pi\eta_0 R \quad (2)$$

in a solvent of viscosity η_0 such as to guarantee consistency of the averages $\langle \dots \rangle$ over force histories $\xi(t)$ with Gibbs’ canonical ensemble, namely,

$$\langle \xi(t) \rangle = 0, \quad \langle \xi_i(t) \xi_j(0) \rangle = 2k_B T_0 \zeta_0 \delta_{ij} \delta(t). \quad (3)$$

This prescription implements the fluctuation-dissipation theorem for the system comprising the Brownian particle and its solvent at temperature T_0 . Strictly speaking, in view of how it deals with long-ranged and long-lived correlations arising from conservation laws governing the solvent hydrodynamics, this practical and commonplace Markovian description applies only asymptotically for late times [5,6]. Corresponding corrections to Eqs. (2) and (3) have recently been analyzed with single-particle techniques in nanostructured environments [7,8].

Thanks to its prominent role in the “middle world” [2] between the macro- and microcosmos, and its experimental and theoretical controllability, Brownian motion

has become the “drosophila” for formulating and testing new (and sometimes controversial) developments in equilibrium and nonequilibrium statistical mechanics [9–15]. In this Letter, we introduce a nonequilibrium generalization that has so far received little attention, namely, the Brownian motion of a particle maintained at an elevated temperature $T_p > T_0$. From its hypothetical sibling (“cool Brownian motion”, $T_p < T_0$) such “hot Brownian motion” (HBM) is distinguished by having obvious realizations of major technological relevance such as nanoparticles suspended in water and diffusing in a laser focus. Because of a time-scale separation between heat conduction and Brownian motion, these particles carry with them a radially symmetric hot halo. This increases the contrast for detection by a second laser, which provides the basis for promising photothermal particle tracking [16] and correlation spectroscopy (“PhoCS”) [17–19] methods with a high potential of complementing corresponding fluorescence techniques [20] in numerous applications. But the heating also gives rise to increased diffusivities [19], a phenomenon that might affect other nanoparticle trapping and tracking setups, too [21–24]. The development of an accurate theoretical description of hot Brownian motion therefore becomes a crucial prerequisite for attaining quantitative control over these emerging technologies. This is not an entirely straightforward task (as some might suggest [25]) and requires an extension of the familiar theory, as explained in the following. We arrive at simple analytical generalizations of Eqs. (2) and (3), which should be sufficiently accurate for most practical applications.

For clarity, we restrict the following discussion to an idealized situation: a hot spherical Brownian particle of radius R at the center of a comoving coordinate system in a solvent with a temperature-dependent viscosity $\eta(T)$ that attains the value η_0 at the ambient temperature T_0 imposed at infinity. Favorable conditions are assumed, such that potential complications resulting from long-time tails [8], convection [26], thermophoresis [27], etc., can be neglected. We do however distinguish the solvent temperature T_s at the hydrodynamic boundary corresponding to the

particle surface from the particle temperature T_p itself, as these may differ substantially [28]. It is the temperature difference $\Delta T \equiv T_s - T_0$ that determines the heat flux responsible for the nonequilibrium character of the problem. On relevant time scales, the resulting temperature field around the particle follows from the stationary heat equation, i. e.

$$T(r) = T_0 + R\Delta T/r. \quad (4)$$

The task of finding appropriate generalizations of Eqs. (2) and (3) under these conditions is split into two steps corresponding to the two force terms in Eq. (1), the damping and the driving force, or friction and thermal noise, respectively.

The first goal is mainly technical, namely, to generalize Eq. (2) by solving

$$\nabla \cdot \mathbf{u} = 0, \quad \nabla p = \nabla \cdot \eta(r)[\nabla \mathbf{u} + (\nabla \mathbf{u})^T] \quad (5)$$

for the stationary fluid velocity field $\mathbf{u}(\mathbf{r})$ under the usual no-slip boundary condition. The new feature compared to Stokes' classical derivation is the radially varying viscosity $\eta(r)$ resulting from Eq. (4). A numerically precise solution of Eq. (5) can be obtained with a differential shell method [29] along the lines of similar work for inhomogeneous elastic media [30]. However, for our present purposes, as well as for practical applications, we wish to find a generally applicable analytically tractable approximation. We therefore resort to a toy model that evades the technical difficulties related to the vector character of the fluid velocity but retains the long-ranged nature of the hydrodynamic flow field [31]. We replace $\mathbf{u}(\mathbf{r})$ by a fictitious diffusing scalar $u(\mathbf{r})$ without direct physical significance, for which Eq. (5) is readily solved analytically. More explicitly, Eq. (5) reduces to $\nabla \cdot \eta(r)\nabla u(\mathbf{r}) = 0$ in the scalar model. A separation ansatz $u(\mathbf{r}) = u_r(r)u_\vartheta(\vartheta)$ leads to the radial equation

$$[\partial_r + 2/r + (\partial_r \ln \eta)]\partial_r u_r = 0 \quad (6)$$

solved by $\partial_r u_r \propto (\eta r^2)^{-1}$ for physically reasonable functions $\eta(r)$. The quantities u_r and $\eta \partial_r u_r$ are now interpreted as the analogue of the fluid velocity and the hydrodynamic drag force per area, respectively. The generalized effective friction coefficient ζ_{HBM} of hot Brownian motion is then estimated up to a numerical factor as their ratio, disregarding the contribution from the angular part. A comparison with Eq. (2) in the isothermal limiting case of constant viscosity $\eta(r) = \eta_0$ helps to calibrate the model and fix the undetermined numerical factor, which is then taken over to situations with radially varying $\eta(r)$. The accuracy of this procedure can be assessed and further improved by a comparison with analytical and numerical results from the aforementioned differential shell method [29]. Some technical details are provided in [32] and the result is summarized in Fig. 1.

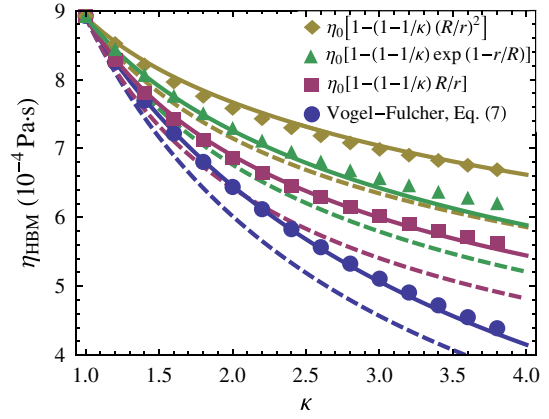


FIG. 1 (color online). Effective viscosity η_{HBM} (scaled to the value for water at $\kappa = 1$) for exemplary long-ranged radial viscosity profiles $\eta(r)$ with $\kappa \equiv \eta_0/\eta(r=R)$ in a parameter regime of potential practical interest. Analytical predictions of the scalar toy model are compared to numerical results from the differential shell method (symbols). While the simplest version of the model (dashed lines), which employs a constant calibration factor, exhibits noticeable systematic errors, the more elaborate version (solid lines), should be sufficiently accurate for practical applications. The lowest solid curve corresponds to Eq. (8).

An analytically tractable expression for the effective friction coefficient ζ_{HBM} as a function of temperature finally results from a combination of the calibrated model with Eq. (4) and a phenomenological expression for the temperature dependence of the solvent viscosity such as

$$\eta(T) = \eta_\infty \exp[A/(T - T_{\text{VF}})] \quad (7)$$

(e.g. for water). The effective friction can be reinterpreted in terms of an effective solvent viscosity $\eta_{\text{HBM}} \equiv \zeta_{\text{HBM}}/6\pi R$ that replaces η_0 in Eq. (2) under nonisothermal conditions. For reduced temperature increments $\theta \equiv \Delta T/(T_0 - T_{\text{VF}}) < 1$ the result is well approximated by its truncated Taylor series [32]

$$\frac{\eta_0}{\eta_{\text{HBM}}} \approx 1 + \frac{193}{486} \left[\ln \frac{\eta_0}{\eta_\infty} \right] \theta - \left[\frac{56}{243} \ln \frac{\eta_0}{\eta_\infty} - \frac{12563}{118098} \ln^2 \frac{\eta_0}{\eta_\infty} \right] \theta^2. \quad (8)$$

This provides the wanted generalization of Eqs. (1) and (2).

To turn Eqs. (1)–(3) into a fully predictive Markov model of hot Brownian motion, the remaining task is to compute, from both the viscosity and temperature profiles, $\eta(r)$ and $T(r)$, the appropriate effective temperature T_{HBM} that accounts for the modified spectrum of thermal forces in the vicinity of the particle and replaces T_0 in Eq. (3). In other words, we aim at establishing a generalized nonequilibrium fluctuation-dissipation relation for Brownian motion in a comoving radial temperature gradient. In analogy to the better understood situation in globally isothermal nonequilibrium steady states [33], we expect to retrieve the fluctuation-dissipation relation only after excluding the “housekeeping heat“ from the entropy balance; i.e.,

the heat constantly flowing from the particle to infinity to maintain the temperature gradient. All we have to consider is the minuscule excess dissipation associated with the damped motion of the Brownian particle. In this respect, it is crucial to appreciate the long-range correlated character of the hydrodynamic flow, which affects both dissipation and thermal fluctuations. It also helps in setting up a systematic coarse-grained calculation by extending the standard framework of fluctuating hydrodynamics [34] to moderate temperature gradients [29].

As pointed out by Einstein [3], the process of Brownian motion can be understood as a detailed balance of antagonistic fluxes. In particular, energy is continuously transferred from the solvent to the particle and vice versa; i.e., it is transformed from thermal into kinetic energy and back. In a stationary situation the mutual energy transfer must be balanced to obey the first law. Moreover, to obey the second law, it must not cause a net average entropy change, which was the origin of major reservations against the modern interpretation of Brownian motion till the early 20th century. More precisely, the spatial integral over the local excess dissipation $\dot{q}(\mathbf{r})$ —i.e., the heat created (per unit of time) by the solvent flow at position \mathbf{r} in response to the movement of the Brownian particle—must on average match the rate of kinetic energy transfer \dot{W}_p to the particle,

$$\langle \dot{W}_p \rangle = \int d\mathbf{r} \langle \dot{q}(\mathbf{r}) \rangle. \quad (9)$$

And, to respect the second law, one has to require that the integral over the local entropy flux to the solvent—i.e., the local dissipation rate $\dot{q}(\mathbf{r})$ divided by the local solvent temperature $T(\mathbf{r})$ —equals on average the entropy flux $\dot{S}_p = \dot{W}_p/T_{\text{HBM}}$ conferred to the Brownian particle:

$$\int d\mathbf{r} \frac{\langle \dot{q}(\mathbf{r}) \rangle}{T(\mathbf{r})} = \frac{1}{T_{\text{HBM}}} \int d\mathbf{r} \langle \dot{q}(\mathbf{r}) \rangle. \quad (10)$$

This then defines the wanted effective Brownian temperature T_{HBM} , if the dissipation $\dot{q}(\mathbf{r})$ is expressed in terms of the local viscosity $\eta(\mathbf{r})$ and $\nabla \mathbf{u}(\mathbf{r})$. Within our scalar model $\dot{q}(\mathbf{r}) = 2\eta(r)\{\partial_r u_r(r)\}^2$ [32], hence

$$T_{\text{HBM}} = \int d\mathbf{r} \eta(r) \langle (\partial_r u_r)^2 \rangle / \int d\mathbf{r} \frac{\eta(r)}{T(r)} \langle (\partial_r u_r)^2 \rangle. \quad (11)$$

Note that both the viscosity and temperature profiles, $\eta(r)$ and $T(r)$, enter explicitly. For the special case of a temperature-independent constant viscosity η_0 this reduces to the simple explicit expression

$$T_{\text{HBM}} = \Delta T / \ln(1 + \Delta T/T_0). \quad (12)$$

The analytical expression generalizing this to the main case of interest, a viscosity $\eta(r)$ that varies radially according to Eqs. (4) and (7), is given in Ref. [32]. For small temperature increments $\Delta T \ll T_0$ a practical approximation is

$$T_{\text{HBM}} \approx T_0 + \Delta T/2 - [1 - \ln(\eta_0/\eta_\infty)]\Delta T^2/(24T_0). \quad (13)$$

A hot Brownian particle described by Eqs. (2) and (3) with η_0 and T_0 replaced by the corresponding effective quantities η_{HBM} and T_{HBM} from Eqs. (8) and (13) performs a random diffusive motion characterized by an effective diffusion coefficient D_{HBM} obeying the generalized Stokes-Einstein relation

$$D_{\text{HBM}} = \frac{k_B T_{\text{HBM}}}{6\pi\eta_{\text{HBM}}R}. \quad (14)$$

This prediction is tested against the numerical differential shell method in the inset of Fig. 2. The good agreement demonstrates the equivalence of Eqs. (10) and (11).

In order to test Eq. (14) also experimentally, we used a photothermal microscopy setup with gold nanoparticles in water, as described in Refs. [19,32]. Particles passing through the common focal volume of a heating and a detection laser beam leave a trace of photothermal bursts in the detector, which encodes information about the diffusivity. The spatially inhomogeneous heating power in the laser focus implies, via Eq. (14), that the diffusion in the focus is inhomogeneous [35]. We therefore pursue a first-passage time approach to determine the apparent effective diffusion coefficient \bar{D}_{HBM} of inhomogeneous hot Brownian motion from the burst durations, which we identify with the transit times of the particles passing through the focus volume [32]. The time periods τ during which the photothermal signal supersedes a fixed percent-

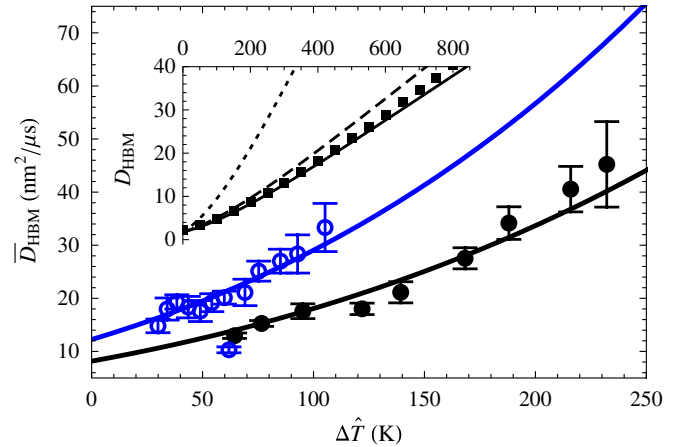


FIG. 2 (color online). The effective diffusion coefficient $\bar{D}_{\text{HBM}}(\Delta \hat{T})$ of hot gold nanoparticles traversing a Gaussian laser focus in water: experimental data (open/closed symbols for $R = 20/30$ nm) versus analytical predictions from the scalar model (solid lines); $\Delta \hat{T}$ is the surface temperature increment for a particle in the center of the focus (see main text); for solvent and focus parameters and the error bars see Ref. [32]. Inset: $D_{\text{HBM}}(\Delta T)$ for homogeneous HBM according to numerical predictions from the differential shell method (squares), analytical solutions of the scalar model (corresponding to the lowest pair of curves in Fig. 1), and the naive suggestion to identify the HBM parameters with the conditions at the particle surface (dotted); the agreement between the symbols and the solid line demonstrates the equivalence of Eqs. (10) and (11).

age of the maximum signal at a given laser power are recorded for a large number of photothermal bursts. The diffusion coefficient is then extracted from the exponential decay of the obtained transit time distribution $P(\tau)$ at large τ [36,37],

$$\ln P(\tau \rightarrow \infty) \propto -\bar{D}_{\text{HBM}}\tau. \quad (15)$$

Figure 2 shows the result of such measurements for various laser powers. The surface temperatures $\hat{T}_s = T_0 + \Delta\hat{T}$ for particles at the center of the laser focus have been calculated from known quantities, namely, the incident laser intensity, the optical absorption coefficient of the particles, and the heat conductivity of the solvent [19]. Because of our limited knowledge of the focus geometry, the factor of proportionality in Eq. (15) could not be determined precisely, though. We therefore took the liberty to multiply each data set by an overall factor to optimize the fit [32]. Yet, the good agreement of the functional dependence with the prediction provides strong support for our analytical results, over a considerable temperature range. At the same time, it establishes hot Brownian motion as a manageable tracer technique.

In summary, by introducing appropriate effective friction (viscosity) and temperature parameters ζ_{HBM} (η_{HBM}) and T_{HBM} , for which we provided explicit analytical expressions in Eqs. (8) and (13), the convenient Markovian description of Brownian motion in terms of Eqs. (2) and (3) could be extended to nonequilibrium conditions, where the temperature of the Brownian particle differs from that of the solvent. While Eqs. (2) and (3) are recovered in the isothermal limit, the general predictions differ significantly from what might have been guessed from simple rules of thumb and provide an instructive illustration of the general dictum that hydrodynamic boundary conditions should not be confused with the microscopic conditions at the boundary [25]. We sidestepped some technical difficulties of the corresponding problem in fluctuating hydrodynamics by introducing an analytical toy model that we calibrated with more elaborate analytical and numerical calculations. Our analytical prediction for the effective diffusion coefficient, based on the generalized Stokes-Einstein relation in Eq. (14), compares favorably with our measurements of gold nanoparticles depicted in Fig. 2 and thus provides a convenient basis for photothermal tracer and particle trapping and tracking techniques with a high potential of complementing corresponding fluorescence-based methods applied in many fields from nanotechnology to biology.

We acknowledge helpful discussions with A. Würger, and financial support from the Deutsche Forschungsgemeinschaft (DFG) via FOR 877.

*kroy@itp.uni-leipzig.de

[1] E. Frey and K. Kroy, *Ann. Phys. (Leipzig)* **14**, 20 (2005).

- [2] M. Haw, *Middle World: The Restless Heart of Matter and Life* (Macmillan, New York, 2006).
- [3] A. Einstein, *Ann. Phys. (Berlin)* **322**, 549 (1905).
- [4] M. Haw, *Phys. World* **18**, 19 (2005).
- [5] J. A. McLennan, *Introduction to Non-Equilibrium Statistical Mechanics* (Prentice Hall, Englewood Cliffs, 1988).
- [6] P. Keblinski and J. Thomin, *Phys. Rev. E* **73**, 010502 (2006).
- [7] S. Martin, M. Reichert, H. Stark, and T. Gisler, *Phys. Rev. Lett.* **97**, 248301 (2006).
- [8] S. Jeney *et al.*, *Phys. Rev. Lett.* **100**, 240604 (2008).
- [9] V. Blicke *et al.*, *Phys. Rev. Lett.* **96**, 070603 (2006).
- [10] V. Blicke *et al.*, *Phys. Rev. Lett.* **98**, 210601 (2007).
- [11] J. R. Howse *et al.*, *Phys. Rev. Lett.* **99**, 048102 (2007).
- [12] F. Ritort, *Adv. Chem. Phys.* **137**, 31 (2008).
- [13] J. Dunkel and P. Hänggi, *Phys. Rep.* **471**, 1 (2009).
- [14] D. Speer, R. Eichhorn, and P. Reimann, *Phys. Rev. Lett.* **102**, 124101 (2009).
- [15] F. Jülicher and J. Prost, *Eur. Phys. J. E* **29**, 27 (2009).
- [16] S. Berciaud, L. Cognet, G. A. Blab, and B. Lounis, *Phys. Rev. Lett.* **93**, 257402 (2004).
- [17] V. Octeau *et al.*, *ACS Nano* **3**, 345 (2009).
- [18] P. M. R. Paulo *et al.*, *J. Phys. Chem. C* **113**, 11451 (2009).
- [19] R. Radünz, D. Rings, K. Kroy, and F. Cichos, *J. Phys. Chem. A* **113**, 1674 (2009).
- [20] S. A. Kim, K. G. Heinze, and P. Schwille, *Nat. Methods* **4**, 963 (2007).
- [21] P. M. Hansen, V. K. Bhatia, N. Harrit, and L. Oddershede, *Nano Lett.* **5**, 1937 (2005).
- [22] H. Cang *et al.*, *Appl. Phys. Lett.* **88**, 223901 (2006).
- [23] D. Lasne *et al.*, *Biophys. J.* **91**, 4598 (2006).
- [24] X. Nan, P. A. Sims, and X. S. Xie, *Chem. Phys. Chem.* **9**, 707 (2008).
- [25] A common suggestion is to replace the ambient temperature T_0 and viscosity η_0 by T_s and $\eta(T_s)$, respectively.
- [26] D. Katoshevski, B. Zhao, G. Ziskind, and E. Bar-Ziv, *J. Aerosol Sci.* **32**, 73 (2001).
- [27] Y. Dolinsky and T. Elperin, *J. Appl. Phys.* **93**, 4321 (2003).
- [28] S. Merabia *et al.*, *Proc. Natl. Acad. Sci. U.S.A.* **106**, 15113 (2009).
- [29] D. Rings *et al.* (unpublished).
- [30] A. J. Levine and T. C. Lubensky, *Phys. Rev. E* **65**, 011501 (2001).
- [31] D. Frenkel, in *Soft Condensed Matter Physics in Molecular and Cell Biology*, edited by W. Poon and D. Andelman (Taylor & Francis, New York, 2006), p. 19f.
- [32] See supplementary material at <http://link.aps.org/supplemental/10.1103/PhysRevLett.105.090604>.
- [33] M. Baiesi, C. Maes, and B. Wynants, *Phys. Rev. Lett.* **103**, 010602 (2009).
- [34] E. H. Hauge and A. Martin-Löf, *J. Stat. Phys.* **7**, 259 (1973).
- [35] A wider focus of the heating laser would avoid this complication but is generally undesirable as one wants to minimize sample irradiation.
- [36] D. S. Ko *et al.*, *Chem. Phys. Lett.* **269**, 54 (1997).
- [37] A. Nagar and P. Pradhan, *Physica (Amsterdam)* **320A**, 141 (2003).